Published in final edited form as:

J Phys Chem B. 2013 December 19; 117(50): 15935–15942. doi:10.1021/jp407321g.

Two-Photon Fluorescence Spectroscopy and Imaging of 4-Dimethylaminonaphthalimide-Peptide and Protein Conjugates

Alan M. McLean[a], **Elke Socher**[b], **Oleg Varnavski**[a], **Travis B. Clark**[a], **Barbara Imperiali**[b], and **Theodore Goodson III**[a]

Barbara Imperiali: imper@mit.edu; Theodore Goodson: tgoodson@umich.edu

[a]Department of Chemistry, University of Michigan, Ann Arbor, Michigan 48109

[b]Departments of Chemistry and Biology, Massachusetts Institute of Technology, Cambridge, Massachusetts 02139

Abstract

We report detailed photophysical studies on the two-photon fluorescence processes of the solvatochromic fluorophore 4-DMN as a conjugate of the important calmodulin (CaM) and the associated CaM-binding peptide M13. Strong two-photon fluorescence enhancement has been observed which is associated with calcium binding. It is found that the two-photon absorption cross-section is strongly dependent on the local environment surrounding the 4-DMN fluorophore in the CaM conjugates, providing sensitivity between sites of fluorophore attachment. Utilizing time-resolved measurements, the emission dynamics of 4-DMN under various environmental (solvent) conditions are analyzed. In addition, anisotropy measurements reveal that the 4-DMN-S38C-CaM system has restricted rotation in the calcium-bound calmodulin. To establish the utility for cellular imaging, two-photon fluorescence microscopy studies were also carried out with the 4-DMN-modified M13 peptide in cells. Together, these studies provide strong evidence that 4-DMN is a useful probe in two-photon imaging, with advantageous properties for cellular experiments.

Keywords

environment sensitive fluorescence; fluorescent amino acid; cellular imaging; two photon spectroscopy; time resolved emission and local electric field

Introduction

In the past decade there have been many important developments in both the synthesis of fluorescent probes and creation of new fluorescence-based methodologies.[1,2] Recently, a family of solvatochromic dyes including dialkylamino-substituted phthalimide and naphthalimide derivatives has been adapted as biological probes to detect protein interactions and conformational changes.[3–8] In the previous studies, one-photon methodologies were utilized to analyze how changes in biological environment influenced fluorescence properties including quantum yield or emission profiles. While useful probes have resulted from these studies, there is certainly the potential to develop even more

Correspondence to: Barbara Imperiali, `imper@mit.edu`; Theodore Goodson, III, `tgoodson@umich.edu`.

Supporting Information **Available**: Detailed protocol of two-photon cross-section measurements, plots of the TPA excited fluorescence as a function of the excitation intensity demonstrating quadratic dependence for all systems, estimation of the error bar (standard deviation) for TPA cross-section measurements for low fluorescence quantum yield variants, TPA-excited fluorescence spectra for low fluorescence quantum yield systems. This information is available free of charge via the Internet at http://pubs.acs.org

sensitive (and spatially selective) methods of fluorescence-based detection. One such approach is the application two-photon excited fluorescence (TPEF) techniques.

TPEF has been shown to be a sensitive tool for probing the excited-state of organic molecules and correlating structure-function relationships.[9–16] Due to the power of this method, two-photon excited processes have been used as a tool for fluorescence-based imaging as well as the foundation for sensitive methods for monitoring aggregation and conformational changes in biomolecules.[17,18] In this case, the information obtained by the two-photon technique has proven to be inaccessible by linear optical methods. Furthermore, two-photon excitation has superior sensitivity to changes in transition dipole moments of the excited fluorophore, as well as greater spatial focusing and depth penetration relative to one-photon excitation, and a reduced probability of autofluorescence (scattering) as well as photodamage.[19,20] While two-photon-based methodologies have been investigated for a number of biomolecular processes and compared to one-photon fluorescence processes, there are many important questions that remain in regards to their functionality in diverse biological applications.

Calmodulin (CaM) is a 148 amino acid signaling protein that is responsive to calcium ion fluxes and that regulates more than 30 enzymes and affects virtually all biological processes.[21,22] To function, CaM utilizes a pair of structural motifs called EF-hands. The EF-hand motifs bind calcium ions, causing the N- and C-termini of CaM to bury into distinct hydrophobic pockets thereby exposing a methionine-rich hydrophobic patch on the protein.[23] This exposed hydrophobic patch allows CaM to bind to and activate other proteins. To underscore its importance, CaM is the primary Ca^{2+}-binding protein expressed in the human genome.[21]

Various organic fluorophores have been used to probe protein-protein interactions and the ion binding properties of calmodulin.[3,4] Of particular interest to the current study, the 4-N-N-dimethylamino-1,8-naphthalimide (4-DMN) solvatochromic fluorophore has been applied to CaM and its peptide binding partner M13 in the presence and absence of calcium.[3] For example, an amino acid analog including 4-DMN has been integrated into M13 to monitor CaM-M13 interactions in the presence and absence of Ca(II).[3] Later, a series of cysteine-reactive derivatives were developed to enable selective protein labeling, which was first demonstrated with CaM.[4] In this case, the targeted bioconjugation of CaM with 4-DMN also enabled the development of a sensitive system for calcium detection. Ultimately, the direct introduction of 4-DMN amino acids into peptides and reagents for protein labeling with Cys-reactive 4-DMN derivatives resulted in general approaches for ligand-induced fluorescent enhancement through tertiary structure modulations that alter the local environment of the 4-DMN fluorophore.[3,4]

Single-photon emission spectra have been reported and demonstrate the photophysical behavior of 4-DMN in these calmodulin systems.[3,4] For example, the 4-DMN-M13 peptide calmodulin system exhibits ∼140-fold fluorescence signal enhancement in the presence of calcium-bound CaM.[3] Similarly, direct cysteine labeling to afford specific 4-DMN-CaM covalent conjugates exhibit fluorescence signal enhancements upon calcium addition from ∼5-fold to ∼130-fold, depending on the site where the 4-DMN is covalently attached to CaM.[4] It has been suggested that solvent polarity, solvent relaxation rates, orientation to electric fields, and environmental rigidity influence the observed fluorescence lifetime and/or quantum yield of the 4-DMN fluorophore.[3,4] However, a detailed quantification of absorption and emission properties has not yet been conducted in these systems. In order to optimize functionality of the 4-DMN fluorophore, there are a number of photophysical questions that must be addressed. How does the 4-DMN environment in the calmodulin system influence absorption and emission? Why are certain sites of 4-DMN attachment

better than others? And while previous studies incorporating 4-DMN have utilized a one-photon regime,[3–6] whether it might be possible for to exploit application of approaches in the two-photon regime to enhance signal sensitivity and later imaging.

In this study we investigate the two-photon effects of three 4-DMN calmodulin variants. To examine absorption, 4-DMN-M13 + CaM (Figure 1A), 4-DMN-S38C-CaM (Figure 1B), and 4-DMN-E11C-CaM (Figure 1B) two-photon cross-sections in the presence and absence of calcium are reported. Quantum yield measurements of all variants are reported and time-correlated single photon counting (TCSPC) is utilized to analyze the fluorescence dynamics of 4-DMN-S38C-CaM. We further demonstrate the ability to employ two-photon emission spectroscopy to image the calcium-dependent binding of the 4DMN-M13 peptide to endogenous CaM in live HeLa cells.

II. Experimental

A. Materials

The wild type CaM, 4-DMN-M13, and CaM-4DMN mutant derivatives (S38C, E11C) were prepared according to previously reported protocols.[3,4] In particular, the CaM-S38C and CaM-E11C mutants were selected because these systems exhibited diverse fluorescence enhancements thereby providing systems with different signals to test the sensitivity for future potential applications.[4] Ethylene glycol tetraacetic acid (EGTA) was added to chelate excess calcium for the non-calcium control. For the CaM + 4-DMN-M13 protein-peptide system, final conditions were 3.3 μL of 1.5 M CaM, 2.0 μL of 1.0 M 4-DMN-M13, 2.0 μL of 200 M $CaCl_2$ or 1.0 μL of 50 M EGTA, with tris-buffered saline (TBS), (pH 7.4) constituting the final 200 μL. For CaM-4DMN Cys conjugates, final conditions were 6 μL of 1.5 M CaM, 1.2 μL of 200 M $CaCl_2$ or 1.0 μL of 50 M EGTA, with TBS constituting the final 200 μL. Samples were pipetted into a 50-μL micro-cuvette for all experiments.

B. Photophysical studies

One-photon spectroscopy studies were performed using a FluoroMax-2 Fluorometer with an integration time of 0.100 s and slits set at 2 nm. All emission scans were performed at 420 nm excitation while scanning 450-800 nm emission. Quantum yield was determined by integrating the absolute fluorescence intensity from the emission scan of each sample. This integrated value was compared to the integrated absolute fluorescence intensity of a Coumarin 307 standard dissolved in methanol ($\phi_{497\ nm} = 0.95 \pm 0.02$) and Coumarin 153 dissolved in ethanol ($\phi_{402\ nm} = 0.544 \pm 0.03$).[24,25]

Time-Correlated Single Photon Counting (∼1 ns resolution) was performed using a Tsunami Ti:Sapphire laser with pulses of ∼20 fs width mode-locked at 840 nm. Using a cavity dumper, the beam exits the laser cavity with a repetition rate of 755 kHz. Average pulse energy is ∼13 nJ. A BBO crystal converts the 840 nm pulsed light into 420 nm excitation pulses. The fluorescence from the sample is collected at 500 nm to a right angle of excitation. Time resolution is created by using a Time to Amplitude Converted (TAC), a linear ramp generator. Detailed procedures can be is found in previously published work.[18,26]

Two-Photon Spectroscopy was performed using a mode-locked Ti:sapphire laser delivering ∼30-fs output pulses at a repetition rate of 90 MHz. All emission scans were performed at 800 nm excitation while scanning 450-700 nm emission. Two-photon power dependent fluorescence intensity was utilized to determine two-photon absorption cross-section through the TPEF method.[27,28] Input power from the laser was varied using a variable neutral density filter. The emission detection wavelength during the power dependence scan was selected by the emission wavelength that produced the highest number of counts at 800

nm excitation. Coumarin 307 dissolved in methanol was used as a standard ($(\phi\delta)_{800\ nm}$ = 15 GM).[27] Special attention was paid to suppressing any spurious signals such as scattered light, possible fluorescence impurities etc. (see Supporting Information for details).

C. Cellular imaging studies

HeLa cells were obtained in DMEM (without phenol red) supplemented with 10% FBS, 1 mM glutamine, and 1% penicillin/streptomycin in a humid incubator at 37°C and 5% CO_2. Cells subjected to imaging were seeded in 35 mm glass-bottom dishes at 70-80% confluence in DMEM lacking phenol red. Cells were incubated with 4DMN-labeled M13 peptide for 12 h and immediately before imaging cells were washed with PBS followed by adding DMEM containing 5 mM ionomycin and 2 μM $CaCl_2$ or 5 mM ionomycin and 1 μM EGTA (no calcium), respectively. Images were acquired at 37°C using a Zeiss LSM 710 NLO laser scanning confocal microscope with an inverted microscope platform and 20× objective with a resolution of 512×512 pixels. For one-photon excitation microscopy a 488 nm (Argon laser) was used for excitation and the fluorescence was detected in the range of 500-540 nm. For two-photon excitation microscopy an ultra II femtosecond pulsed-IR laser at 780 nm was used for excitation of 4-DMN and the emission was measured in the range of 500 – 540 nm. Incubation of the cells with 4-DMN-labeled M13 peptide without pretreatment with ionomycin resulted in a weaker fluorescence signal increase since endogenous Ca^{2+} is already present in the cells.

III. Results and Discussion

One-Photon Spectroscopy

Shown in Figure 2 are the one-photon emission spectra for the calmodulin-peptide (4DMN-M13) and ion-binding fluorescent systems (E11C, S38C). In all cases, the 400nm excitation was used. As shown in Figure 2, there is fluorescence signal enhancement in the calcium-bound state of CaM. The M13 and S38C systems exhibit approximately equivalent fluorescence enhancements with calcium binding (∼115-fold), whereas the signal for the 4-DMN-modified E11C is considerably less enhanced once calcium is bound (∼8.4-fold). All three samples exhibited relatively low fluorescence quantum yields in the calcium-free state on the order of ∼0.5%. However, for the case of the 4DMN-M13 bound to Ca^{2+}: CaM complex, the quantum yield increased to approximately 20% (see Table 2). The enhancement in the fluorescence signal in the case of the calcium-bound samples is in part explained by the increased quantum yield however, there are more details regarding this process, which may be understood utilizing other more sensitive fluorescence techniques.

B. Two-Photon Spectroscopy

Two-photon emission measurements were performed on the 4-DMN fluorophore in DMF, the CaM + 4-DMN-M13 system, and the CaM-E11C and CaM-S38C direct mutants. Similar to the one photon excitation scheme we observed large calcium-dependent two-photon excited fluorescence enhancement in each of the CaM systems. CaM + 4-DMN-M13 and CaM-S38C systems exhibit fluorescence enhancement on the order of magnitude of ∼81-fold and ∼97-fold under two-photon excitation (Figure 3). Compared to CaM + 4-DMN-M13 and CaM-S38C, CaM-E11C has a smaller order of enhancement (∼7.9-fold), with a comparable calcium-free fluorescence quantum yield. Two-photon excited fluorescence spectra have been observed slightly broadened and red shifted (by ∼1-7nm) in comparison with one-photon excited ones. This small difference is associated with the inhomogeneous broadening of the probe system[29] as well as with the some disturbance of spectrometer calibration with increased slit widths to detect weaker TPA –excited fluorescence.

The relative magnitude of enhancement between calcium-bound and calcium-free samples is statistically significant. Due to several advantages, the key result of obtaining the enhanced fluorescence at longer excitation wavelengths (out of resonance) may advantageously impact future applications. In general, *multi-photon* excitation has advantages over single photon techniques since it utilizes a lower excitation frequency and provides greater focusing at a defined emission wavelength.[19] Due to the excitation wavelength falling into the near IR region, this excitation route possess less scattering and absorption in the tissue.[29] Furthermore, the two-photon cross-section is directly proportional to the square of transition dipole moment as well as to the square of change of the static dipole moment after excitation,[20] and thus these methodologies can detect changes in protein conformation, excited-state dipoles, and charge transfer character with a high degree of sensitivity.[20]

Two-photon absorption cross-sections were measured and compared with 4-DMN in DMF (Table 1). Interestingly, the largest cross-section was obtained for the S38C system. When one takes into account the changes in the quantum yield, the actual two-photon absorption cross-section does not significantly change between calcium-free and calcium-bound M13 and E11C samples. This trend may seem paradoxical, since the effective solvent environment changes when calcium is added.[3,4] The reason can be associated with the fact that the quantum the fluorescence quantum yield is affected by the rate of non-radiative relaxation of the probe in the molecular configuration following the initial Frank-Condon configuration relevant to the instantaneous two-photon absorption process. Calcium change strongly affects this nonradiative decay channel suggestively via transition excited state which was found to be very sensitive to the solvent polarity for a close analog of 4DMN.[37] On the other hand, several studies have shown that two-photon cross-section can be minimally affected by solvent for some fluorophores.[31–33] One sees slightly different trend for the S38C sample, where the cross-section does change upon addition of calcium. This particular system illustrated a number of different properties, which illustrated the sensitivity of the two-photon method (see below).

From measurements with the different variants one might suggest that the two-photon cross-section depends rather strongly on the site of 4-DMN attachment. At the same time, the trend in TPA cross-section is not substantially affected by the calcium change: when going from E11C configuration to the S38C configuration the TPA cross section increases by factor ∼31 for Ca-free systems in comparison with still strong enhancement by factor ∼20.5 for Ca- bound systems. This indicates that the TPA- response and fluorescence quantum yield change with the calcium presence are controlled by different local environment mechanisms affecting different molecular configurations as we mentioned above (see more details below). Site-dependent TPA cross- section changes may be attributable to differences in local static dipole, and local electric field since the two-photon cross-section is dependent on the square of the static dipole difference between the ground and excited state.[20] As Rebane *et al.*[20] characterized for β-barrel structures, the magnitude of the local electric field in proteins can be frequently high, affecting the magnitude of static dipole moment.[20,32,33] Assuming that the 4-DMN fluorophore has an intrinsic change in polarizability between ground and excited state, we can examine local electric field effects on two-photon cross-section in 4-DMN variants. Interestingly, 4-DMN in DMF does not possess large TPA cross –section. This can be associated with the isotropic environment of the probe in this case cancelling out a substantial part of the anisotropic electron density effect.

Depending on the orientation of the local electric field, the dipole moment can either be enhanced or suppressed.[32] Since the 4-DMN-M13 + CaM linker system has an average cross-section of 1.2, approximately 1/4 the magnitude of the 4-DMN control, the local electric field must have an orientation that suppresses the two-photon cross-section. On the other hand, S38C-4DMN-CaM, with an average two-photon cross-section <20, may have a

local electric field with an orientation that enhances the two-photon cross-section. E11C-4-DMN-CaM, with an average two-photon cross-section of 4.7, does not exhibit cross-sectional enhancement or suppression. We can estimate local electric field by assigning acidic amino acids with a whole charge of -1 and basic amino acids with a whole charge of +1.[35] For example, 4-DMN-S38C-CaM is adjacent to a basic arginine residue (PDB: IUP5). Therefore, by assigning arginine with a whole charge value of +1, it is reasonable to suggest that S38C may have a strong local electric field oriented away from the site, resulting in two-photon cross-sectional enhancement.

Conversely, 4-DMN-E11C-CaM is directly adjacent to two neutral amino acids (left: alanine, right: phenylalanine). Additionally, E11C has lysine (+1) and glutamic acid (-1) residues adjacent by 2 and 3 amino acids to the right and two additional glutamic residues (-1) adjacent by 4 and 5 amino acids to the left. Assuming that amino acids in closer proximity contribute more to the local electric field, the presence of the closer lysine residue may negate the presence of the larger number of glutamic acid residues surrounding the E11C site. As a consequence, E11C would not have an effective local electric field, producing a two-photon cross-section comparable to the 4-DMN control. Although we assume that the change in polarizability between ground state and excited state does not change with fluorophore location, theoretical calculations suggest that amino acids can impact polarizability as well.[36]

C. Quantum Yield

For 4-DMN in DMF solvent, we report a quantum yield of 0.288. However in aqueous solvent, the quantum yield of 4-DMN is dramatically reduced. Next, we measured the quantum yield of 4-DMN in calmodulin systems (Table 2). The 4-DMN-S38C-CaM system has the highest calcium-bound quantum yield at 0.26. Furthermore, the S38C calmodulin mutant has the lowest calcium-free quantum yield at 0.002. This, again, suggests this system showing the strongest fluorescence enhancement associated with calcium binding. In contrast, 4-DMN-E11C-CaM has the smallest calcium-bound quantum yield (0.059) and the largest calcium-free quantum yield (0.007) which can be associated with lower non-radiative decay rate for later system.

As a baseline for comparison, we utilized the quantum yields reported for 4-dialkylamino-1,8-naphthalimide (MNP), a close analog of 4-DMN (4-DMN linker replaced with butyl chain).[37] MNP demonstrates quantum yield dependence correlated with solvent polarity.[37] In polar solvents including EtOH and MeOH, the quantum yield was reported at less than 0.01.[37] In non-polar solvents such as hexane, the quantum yield was as high as 0.82.[37] Like MNP, 4-DMN calmodulin variants exhibit sensitive solvent dependence to modulate quantum yield changes. For example, the CaM variants which are calcium free are likely to display 4-DMN, in an open environment, which is exposed to the aqueous, polar solvent, all show has quantum yield values of less than 0.01. These values are even lower than reported QY values for MNP in ethanol, attributable to water-cluster formation.[38] Upon calcium addition, quantum yield increases due to folding, exposing 4-DMN to a more effective hydrophobic environment.[3] To maximize changes in fluorescence efficiency between calcium-bound and calcium-free 4-DMN, one should maximize changes in polarity. Two-photon cross-section does not seem to be significantly dependent in the isotropic solvent polarity. It seems to be an opportunity to disentangle (to some extent) the two-photon absorption properties of 4-DMN from emission characteristics to develop an efficient TPA calcium probe. To gain a deeper understanding of temporal fluorescence emission, time-correlated single-photon counting was performed on 4-DMN (DMF) and 4-DMN-S38C-CaM, the calmodulin derivative with the greatest sensitivity between calcium-bound and non-bound conformations.

D. Time-Correlated Single Photon Counting

The dynamics of the fluorescence was investigated by time-correlated single photon counting on the 4-DMN-S38C-CaM systems, which exhibited the largest two-photon fluorescence sensitivity as discussed above. As seen in Figure 6, calcium-bound 4-DMN-S38C-CaM exhibits the longest decay lifetime, with a single-exponential decay lifetime of 10.2 ± 0.3 ns. Calcium-free 4-DMN-S38C-CaM has showed multi-exponential decay with a dominant fast decaying component with the time constant 64ps (∼98.5% amplitude contribution). We also performed time-correlated single-photon counting on the 4-DMN fluorophore dissolved in DMF, which demonstrated a mono-exponential decay lifetime of 8.2 ± 0.3 ns.

The faster decay rate of calcium-free 4-DMN-S38C-CaM relative to its calcium-bound counterpart is attributable to increased non-radiative decay through multiple relaxation pathways. The nonradiative decay rates can be estimated from the quantum yield and the fluorescence lifetime to be ≈ 0.064ns, 13.8ns for calcium–free system and calcium-added systems, respectively (the major fast decay component in multiexponential decay of 4MN-S38C-CaM+EGPA was used for calculation). These data undoubtedly showed the key role of nonradiative relaxation channel in the fluorescence quantum yield change and calcium sensitivity. An increased rate of nonradiative decay for the model system 1-8-dialkylaminonaphthalimides in polar solvents was suggested to be linked to a stabilized planar transition state, increasing the probability of N4 nitrogen inversion.[37] This can explain much smaller sensitivity of TPA cross-section to the calcium change in comparison with the quantum yield as the former is associated with the ground state molecular configuration. In addition to this, we expect that the elevated rate of the non-radiative decay in aqueous solvent is caused by hydrogen bonding and water cluster formation in the dialkylaminonapthalimides.[38] Because its non-radiative decay is higher, the quantum yield of calcium-free 4-DMN-S38C-CaM is smaller. In contrast, calcium-bound 4-DMN-S38C-CaM has a prolonged lifetime because the fluorophore is more shielded from aqueous solvent and exists in a more non-polar environment. As a consequence to this, calcium-bound 4-DMN-S38C-CaM will have a higher quantum yield. This phenomena is similar to trends observed for the MNP fluorophore, where increasing polarity led to a shortening of lifetime.[37]

Anisotropy measurements reveal a different trend in decay times, as seen in Figure 7 and in Table 3. The anisotropic decay of the 4-DMN fluorophore is very short, within the range of the IRF. Calcium-bound 4-DMN-S38C-CaM has the longest anisotropy decay, with a τ_1 value at 13.3 ± 0.5 ns. Calcium-free 4-DMN-S38C-CaM has a bi-exponential decay, with a τ_1 value of 1.8 ns ± 0.5 ns (A_1 = 0.333) and a τ_2 value of 17.3 ± 1.0 ns (A_2 = 0.067 The long rate of anisotropic decay in calcium-bound 4-DMN-S38C-CaM, on the order of 10+ ns, indicates that the fluorophore has restricted motion.[19] Considering that the fluorophore is tucked into a hydrophobic pocket within the calmodulin architecture, we can infer that the calmodulin folded environment locks the fluorophore into a fixed plane. In contrast, calcium-free 4-DMN-S38C-CaM exhibits a fast component of anisotropic decay combined with a slower component (bi-exponential anisotropic decay). Because the fast component of decay is dominant ($A_1/A_2 \approx 5$), the bulk of calcium-free anisotropic decay exhibits relatively unrestricted rotation.

However, the A_2 component of decay suggests that the calcium-free fluorophore has orientations where rotation is hindered.[19] We propose that these restricted orientations correspond to the linker region, where 4-DMN is covalently attached to the calmodulin peptide. Lastly, our results suggest that 4-DMN fluorophore (DMF) can freely rotate in solution without restriction, explaining its sub-nanosecond anisotropy decay lifetime. We have also performed time resolved measurement for the 4DMN-M13 system using

fluorescence upconversion setup with subpicosecond time resolution.[10] These measurements demonstrated a similar trend in isotropic and anisotropic fluorescence decays as for S38C system (Figure 8)

High residual fluorescence anisotropy for calcium bound 4-DMN-M13-CaM indicates that the fluorophore undergoes highly restricted rotation in this case. This can be associated with locking of the fluorophore in the calmodulin folded environment similar to what was observed for the S38C. At the same time calcium –free *4-DMN-M13* system demonstrated very fast loss of the fluorescence anisotropy resulted from probe rotational motion with minor restrictions. The locking of the chromophore and associated decrease of the nonradiative decay rate seems to play a key role in the fluorescence enhancement in calcium –bound systems investigated in this work.

F. Live cell imaging of endogenous CaM using the 4DMN labeled M13 peptide

To explore the utility of the 4-DMN labeled M13 peptide to sense endogenous CaM in living HeLa cells, we performed a series of imaging experiments using fluorescence microscopy. Therefore living HeLa cells were incubated with the 4-DMN labeled M13 peptide at a 10 μM concentration for 12 h. The M13 peptide is an 18mer peptide with 7 out of 18 amino acid having charged side chains which indicates that the M13 peptide is a cell penetrating peptide.[37] A Ca^{2+} dependent fluorescence change could be monitored by either adding the selective calcium ionophore agent ionomycin and $CaCl_2$ which raises the intracellular level of calcium (see Figure 9A). The addition of ionomycin and EGTA will lead to a decreased intracellular level of calcium. Cells incubated with the 4-DMN labeled M13 peptide showed a faint fluorescence intensity, whereas prompt increase in HeLa cell fluorescence was observed upon addition of ionomycin/$CaCl_2$ (Figure 9B), as determined by widefield microscopy in live HeLa cell samples. We also added ionomycin/EGTA and could observe a decrease in fluorescence (Figure 8C). The sensitivity of the 2P images appeared to be better compared to the 1P images, which show a higher background fluorescence. This can be explained by the fact that in the confocal image a significant proportion of the fluorescence signal that is being collected is autofluorescence, since 4-DMN is being excited at 488 nm. Autofluorescence in 2P microscopy is less pronounced since excitation occurs at 780 nm. The successful imaging of endogenous CaM using the 4DMN-labled M13 peptide proved the ability to use TPEF to detect 4DMN fluorescence in living cells.

IV. Conclusions

In this contribution, we have reported two-photon absorption and emission characteristics of the 4-DMN fluorophore in 4-DMN-M13, CaM-E11C, and CaM-S38C variants. We have observed one-photon excited fluorescence enhancement in the calcium-bound state, corresponding to enhancement in a quantum yield. Utilizing two-photon spectroscopy, we have reported two-photon emission and two-photon cross-sections for 4-DMN-M13, CaM-E11C, and CaM-S38C systems. We have also observed fluorescence enhancement of two-photon excited fluorescence in the calcium-added state. Due to the added benefits of a two-photon methodology, the results suggest that two-photon spectroscopy can provide greater benefits for the 4-DMN fluorophore. We have obtained strong evidence of two-photon cross-section correlation to the location of 4-DMN placement on the calmodulin peptide. Enhancement of two-photon absorption cross-section by a factor up to ∼8.8 for the S38C –attachment configuration as compared to the probe in the reference solution has been observed. This opens the way for two-photon detection and imaging at increased signal-to-noise ratio. From our measurements we infer that 4-DMN in calmodulin exhibits a high rate of non-radiative decay through a stabilized planar conformation in polar solvents. Anisotropy lifetime measurements of S38C-CaM and M13-CaM add to this model; they suggest that the 4-DMN fluorophore is locked in a static, “lock-and-key”, conformation

upon calcium binding. This static conformation would inhibit fluorophore interaction, increasing the extent of radiative decay. This suggests that enhancement between bound and non-bound 4-DMN-calmodulin conformations can be further optimized.

Supplementary Material

Refer to Web version on PubMed Central for supplementary material.

Acknowledgments

TGIII acknowledges the National Science Foundation (DMR-Polymers) for partial support of this research. BI acknowledges the National Institutes of Health (R01 EB 010246). ES was supported by a postdoctoral fellowship from Deutsche Forschungsgemeinschaft (DFG; SO 1100/1-1).

References

1. Lavis LD, Raines RT. Bright Ideas for Chemical Biology. ACS Chem Biol. 2007; 3:142–155. [PubMed: 18355003]
2. Lemke, Ea; Schultz, C. Principles for Designing fluorescent Sensors and Reporters. Nat Chem Biol. 2011; 7:480–3. [PubMed: 21769088]
3. Loving G, Imperiali BA. Versatile Amino Acid Analogue of the Solvatochromic Fluorophore 4-N,N-dimethylamino-1,8-naphthalimide: a Powerful Tool for the Study of Dynamic Protein Interactions. J Am Chem Soc. 2008; 130:13630–8. [PubMed: 18808123]
4. Loving G, Imperiali B. Thiol-Reactive Derivatives of the Solvatochromic 4-N,N-Dimethylamino-1,8-naphthalimide Fluorophore: a Highly Sensitive Toolset for the Detection of Biomolecular Interactions. Bioconj Chem. 2009; 20:2133–41.
5. Zhong C, Mu T, Wang L, Fu E, Qin J. Unexpected Fluorescent Behavior of a 4-amino-1,8-naphthalimide Derived Beta-Cyclodextrin: Conformation Analysis and Sensing Properties. Chem Commun. 2009:4091–3.
6. Fuller, Aa; Seidl, FJ.; Bruno, Pa; Plescia, Ma; Palla, KS. Use of the Environmentally Sensitive Fluorophore 4-N,N-dimethylamino-1,8-naphthalimide to Study Peptoid Helix Structures. Biopolymers. 2011; 96:627–638. [PubMed: 22180910]
7. Wei S, Sun Y, Guo P, Hu X, Fan J. A Novel 4-(tetrahydro-2-furanmethoxy)-N-octadecyl-1,8-naphthalimide Based Blue Emitting probe: Solvent Effect on the Photophysical Properties and Protein Detection. Russian J Bioorg Chem. 2012; 38:469–478.
8. Krueger AT, Imperiali B. Fluorescent Amino Acids: Modular Building Blocks for the Assembly of New Tools for Chemical Biology. Chembiochem. 2013; 14:788–99. [PubMed: 23609944]
9. Bhaskar A, Guda R, Haley MM, Goodson T. Building Symmetric Two-Dimensional Two-Photon Materials. J Am Chem Soc. 2006; 128:13972–3. [PubMed: 17061848]
10. Varnavski O, Yan X, Mongin O, Blanchard-Desce M, Goodson T. Strongly Interacting Organic Conjugated Dendrimers with Enhanced Two-Photon Absorption. J Phys Chem C. 2007; 111:149–162.
11. Bhaskar, a; Ramakrishna, G.; Twieg, RJ.; Goodson, T. Zinc Sensing via Enhancement of Two-Photon Excited Fluorescence. J Phys Chem C. 2007; 111:14607–14611.
12. Brown OJ, Lopez SA, Fuller AO, Goodson T. Formation and reversible dissociation of coiled coil of peptide to the C-terminus of the HSV B5 protein: a time-resolved spectroscopic analysis. Biophys J. 2007; 93:1068–78. [PubMed: 17496024]
13. Williams-Harry M, Bhaskar A, Ramakrishna G, Goodson T, Imamura M, Mawatari A, Nakao K, Enozawa H, Nishinaga T, Iyoda M. Giant Thienylene-Acetylene-Ethylene Macrocycles with Large Two-Photon Absorption Cross Section and Semishape-Persistence. J Am Chem Soc. 2008; 130:3252–3. [PubMed: 18293979]
14. Guo M, Varnavski O, Narayanan A, Mongin O, Majoral J, Blanchard-Desce M, Goodson T. Investigations of Energy Migration in an Organic Dendrimer Macromolecule for Sensory Signal Amplification. J Phys Chem A. 2009; 113:4763–4771. [PubMed: 19317441]

15. Parthasarathy A, Ahn HY, Belfield KD, Schanze KS. Two-Photon Excited Fluorescence of a Conjugated Polyelectrolyte and Its Application in Cell Imaging. ACS Appl Mater Interfaces. 2010; 2:2744–8. [PubMed: 20939595]
16. Oliva MM, Jua R, Ramos M, Segura JL, Cleuvenbergen SVan, Clays K, Goodson T, Lo JT, Casado J. Linear and Nonlinear Optical Properties of Ramified Hexaazatriphenylenes: Charge Transfer Contributions to the Octupolar Response. 2013 submitted.
17. Wang Y, Goodson T. Early Aggregation in Prion Peptide Nanostructures Investigated by Nonlinear and Ultrafast Time-Resolved Fluorescence Spectroscopy. J Phys Chem B. 2007; 111:327–30. [PubMed: 17214480]
18. Wang Y, Clark TB, Goodson T. Two-Photon and Time-Resolved Fluorescence Conformational Studies of Aggregation in Amyloid Peptides. J Phys Chem B. 2010; 114:7112–20. [PubMed: 20429591]
19. Lakowicz, JR. Principles of Fluorescence Spectroscopy. 3rd. Springer; 2006.
20. Drobizhev M, Makarov NS, Tillo SE, Hughes TE, Rebane A. Two-Photon Absorption Properties of Fluorescent Proteins. Nature Meth. 2011; 8:393–9.
21. Means A, VanBerkum M, Bagchi I. Regulatory Functions of Calmodulin. Pharm Therap. 1991; 50:255–270.
22. Black DJ, Tran QK, Persechini A. Monitoring the Total Available Calmodulin Concentration in Intact Cells over the Physiological Range in Free Ca2+ Cell Calcium. 2004; 35:415–25. [PubMed: 15003851]
23. Chin D, Means AR. Calmodulin: a Prototypical Calcium Sensor. Trends Cell Biol. 2000; 10:322–8. [PubMed: 10884684]
24. Lebedkin S, Langetepe T, Sevillano P, Fenske D, Kappes MM. Novel Photophysical Properties of Gold Selenide Complexes: Photogeneration of Singlet Oxygen by [Au 18 Se 8 (dppe) 6] Br 2 and Near-Infrared Photoluminescence of $[Au_{10}Se_4(dpppe)_4]Br_2$. J Phys Chem B. 2002; 106(35): 9019–9026.
25. Rurack K, Spieles M. Fluorescence Quantum Yields of a Series of Red and Near-Infrared Dyes Emitting at 600-1000 nm. Anal Chem. 2011; 83:1232–42. [PubMed: 21250654]
26. Lahankar SA, West R, Varnavski O, Xie X, Goodson T, Sukhomlinova L, Twieg R. Electronic Interactions in a Branched Chromophore Investigated by Nonlinear Optical and Time-Resolved Spectroscopy. J Chem Phys. 2004; 120:337–44. [PubMed: 15267294]
27. Xu C, Webb WW. Measurement of Two-Photon Excitation Cross Sections of Molecular Fluorophores with Data from 690 to 1050 nm. J Opt Soc Amer B. 1996; 13:481.
28. Clark TB, Orr ME, Flynn DC, Goodson T. Synthesis and Optical Properties of Two-Photon Absorbing GFP-type Probes. J Phys Chem C. 2011; 115:7331–7338.
29. Narayanan A, Varnavski OP, Swager TM, Goodson T III. Two Photon Fluorescence Quenching of Conjugated Polymers for TNT Detection. J Phys Chem C. 2008; 112:881–884.
30. Taroni P, Pifferi A, Torricelli A, Comelli D, Cubeddu R. In Vivo Absorption and Scattering Spectroscopy of Biological Tissues. Photochem Photobiol Sci. 2003; 2:124–129. [PubMed: 12664972]
31. Johnsen M, Ogilby PR. Effect of Solvent on Two-Photon Absorption by Vinyl Benzene Derivatives. J Phys Chem A. 2008; 112:7831–9. [PubMed: 18680265]
32. Nag A, Goswami D. Solvent Effect on Two-Photon Absorption and Fluorescence of Rhodamine Dyes. J Photochem Photobiol A, Chemistry. 2009; 206:188–197.
33. Wielgus M, Bartkowiak W, Samoc M. Two-Photon Solvatochromism. I. Solvent Effects on Two-Photon Absorption. Chem Phys Lett. 2012; 554:113–116.
34. Drobizhev M, Tillo S, Makarov NS, Hughes TE, Rebane A. Color Hues in Red Fluorescent Proteins are due to Internal Quadratic Stark Effect. J Phys Chem B. 2009; 113:12860–4. [PubMed: 19775174]
35. Drobizhev M, Scott JN, Callis PR, Rebane a. All-Optical Sensing of the Components of the Internal Local Electric Field in Proteins. IEEE Photonics Journal. 2012; 4:1996–2001.
36. Maroulis G. Computational Aspects of Electric Polarizibility Calculations: Atoms, Molecules, and Clusters. 2006:185–190.

37. Saha S, Samanta A. Influence of the Structure of the Amino Group and Polarity of the Medium on the Photophysical Behavior of 4-Amino-1,8-naphthalimide Derivatives. J Phys Chem A. 2002; 106:4763–4771.

38. Yuan D, Brown RG. Enhanced Nonradiative Decay in Aqueous Solutions of Aminonaphthalimide Derivatives via Water-Cluster Formation. J Phys Chem. 1997; 5639:3461–3466.

39. Gautam A, Chaudhary K, Kumar R, Sharma A, Kapoor P, Tyagi A, Raghava GPS. In Silico Approaches for Designing Highly Effective Cell Penetrating Peptides. J Transl Med. 2013; 11:74. [PubMed: 23517638]

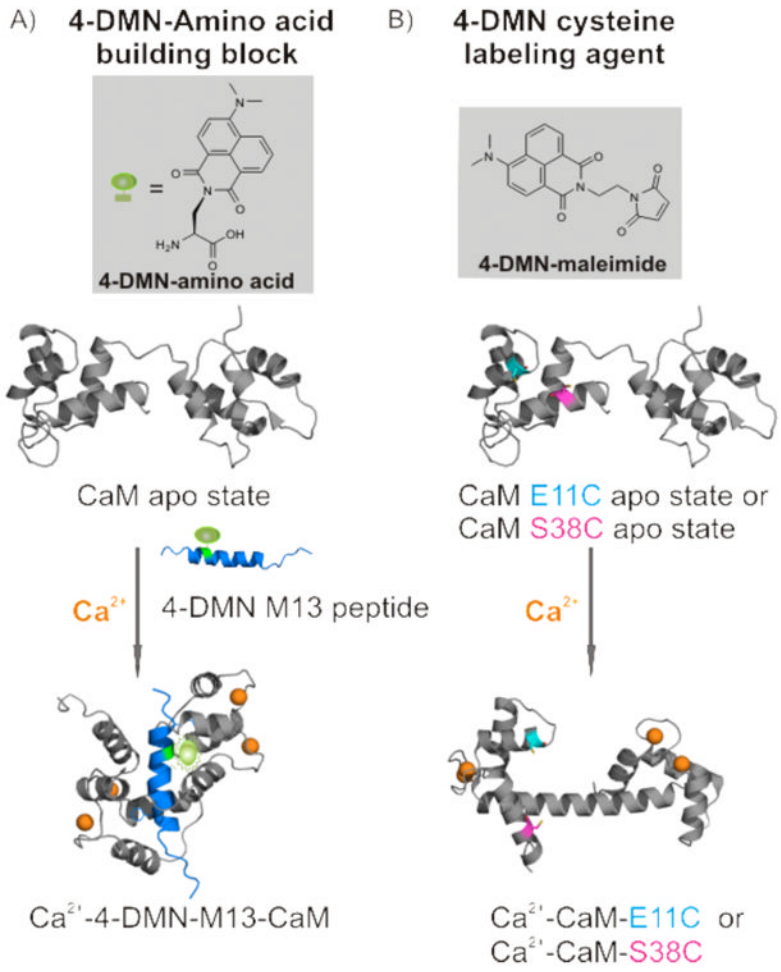

Figure 1.

A) Ca^{2+} activation and binding of CaM (gray) to an M13 peptide mutant (blue) that contains an amino acid with the solvatochromic fluorophore 4-DMN as the side chain. Upon complex formation, 4-DMN exhibits an increase in fluorescence. (PDB of CaM apo state: 1DMO and Ca^{2+}-CaM-M13 complex: 2BBM) B) CaM in the apo state and formation of Ca^{2+} activation of a CaM mutant (gray) with the bound calcium ions indicated by spheres (orange). Both structures indicate the two chosen sites for cysteine mutagenesis E11C and S38C, respectively. Ca^{2+} activation results in burying the attached 4-DMN in either the E11C or the S38C mutant within one of the newly formed hydrophobic pockets, which leads to increased fluorescence. (PDB of CaM apo state: 1DMO and Ca^{2+}-CaM: 1UP5)

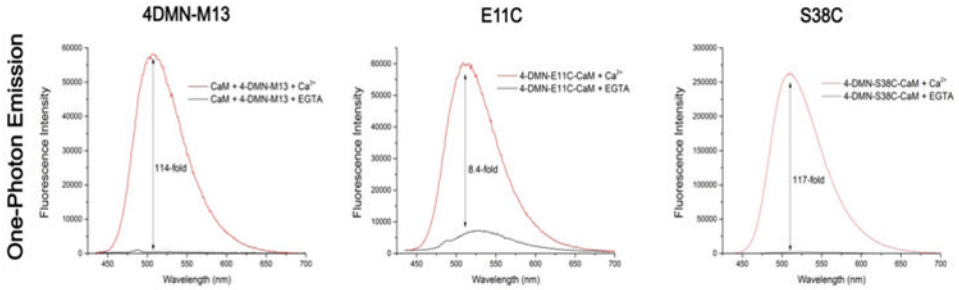

Figure 2.

One-photon emission of 4-DMN-CaM fluorescence systems under calcium-free and calcium-bound conditions at 400 nm excitation.

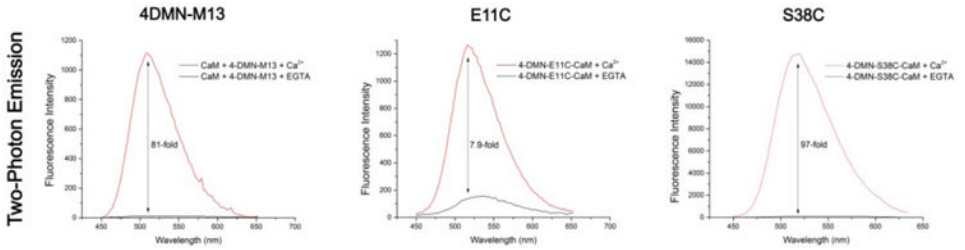

Figure 3.
Two-photon emission of 4-DMN-CaM fluorescent systems under calcium-free and calcium-bound conditions at 800 nm excitation.

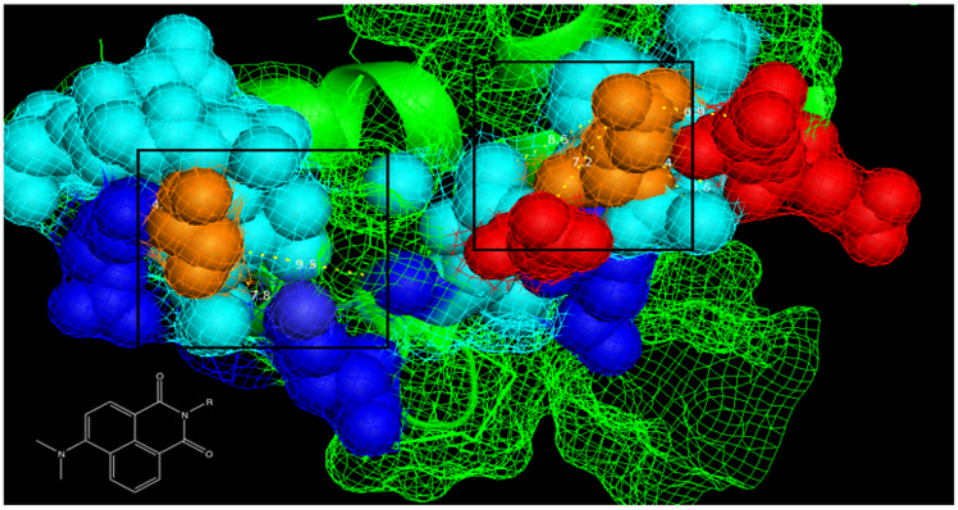

Figure 5.
Crystal structure of S38C (left) and E11C (right) sites on CaM. The orange residue is the site of 4-DMN attachment. Blue residues correspond to basic amino acids. Red residues correspond to acidic amino acids. Cyan residues are neutral amino acids. The 4-DMN fluorophore is tucked into the hydrophobic pocket of the calmodulin protein, folding into the center of the image. Considering that linker length is ∼6 Å and fluorophore length is ∼10 Å, we can approximate fluorophore location at each site (shown by black box).

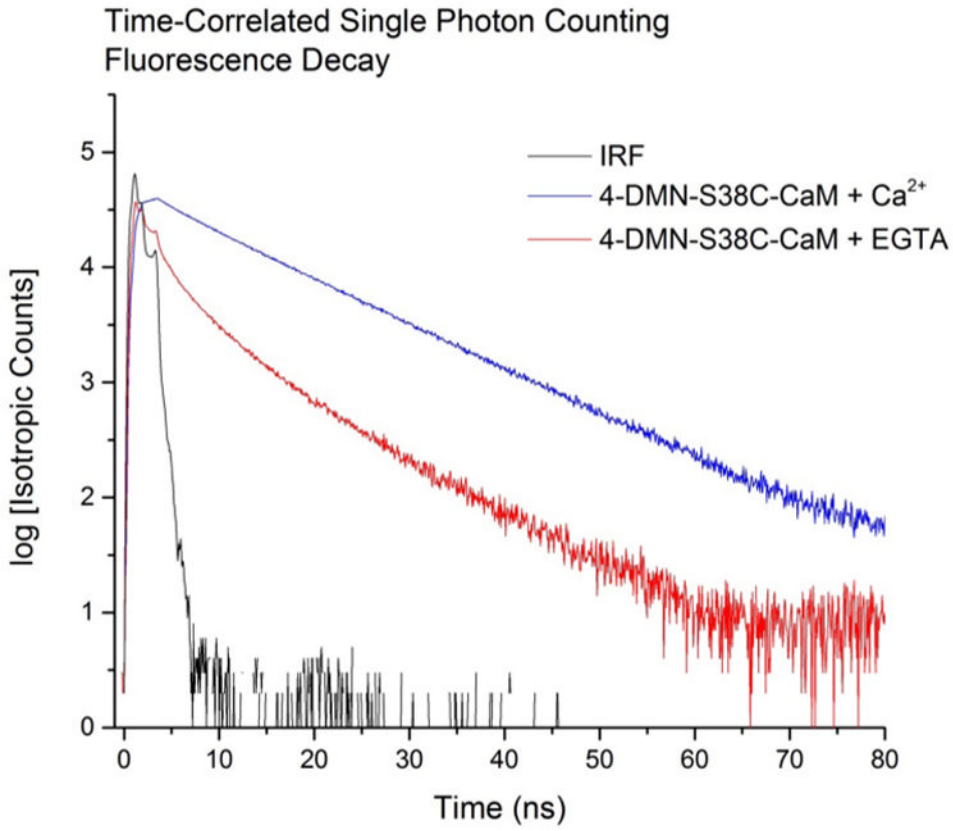

Figure 6.
Time-resolved fluorescence lifetime at 420 nm excitation and 500 nm detection. Best fit results are shown in Table 3.

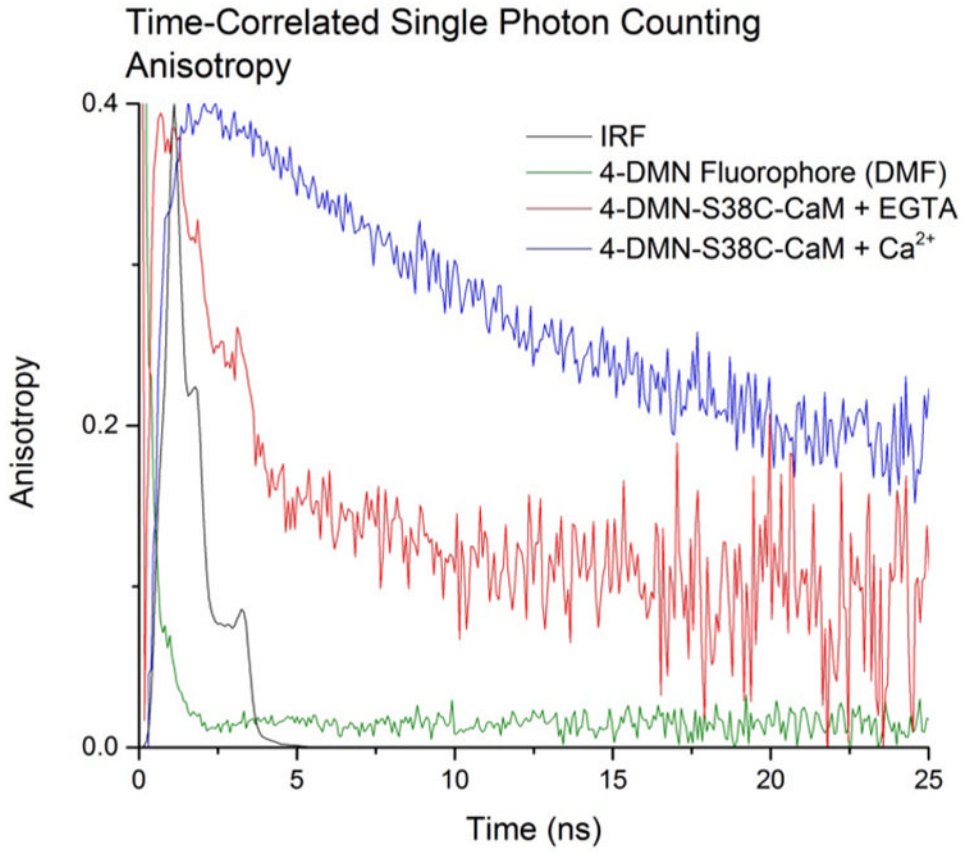

Figure 7.
Time-correlated single photon counting anisotropy at 420 nm excitation and 500 nm detection. Best fit results are shown in Table 3.

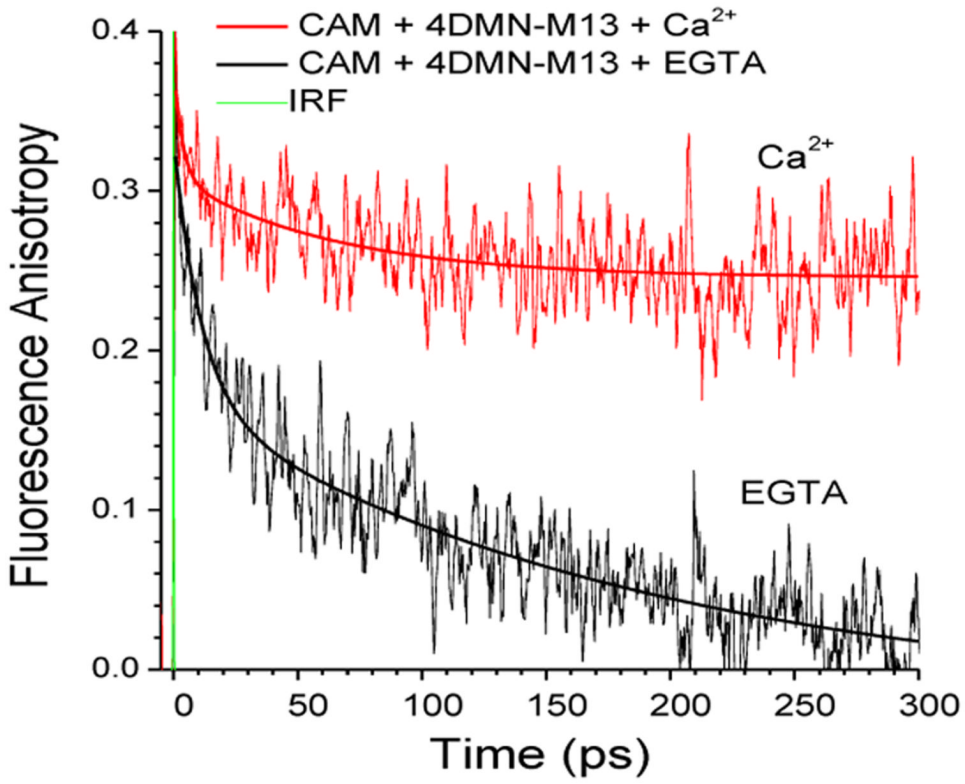

Figure 8. Time-resolved fluorescence anisotropy for 4-DMN-M13 system at 400 nm excitation and 500 nm detection measured with 0.2ps time resolution

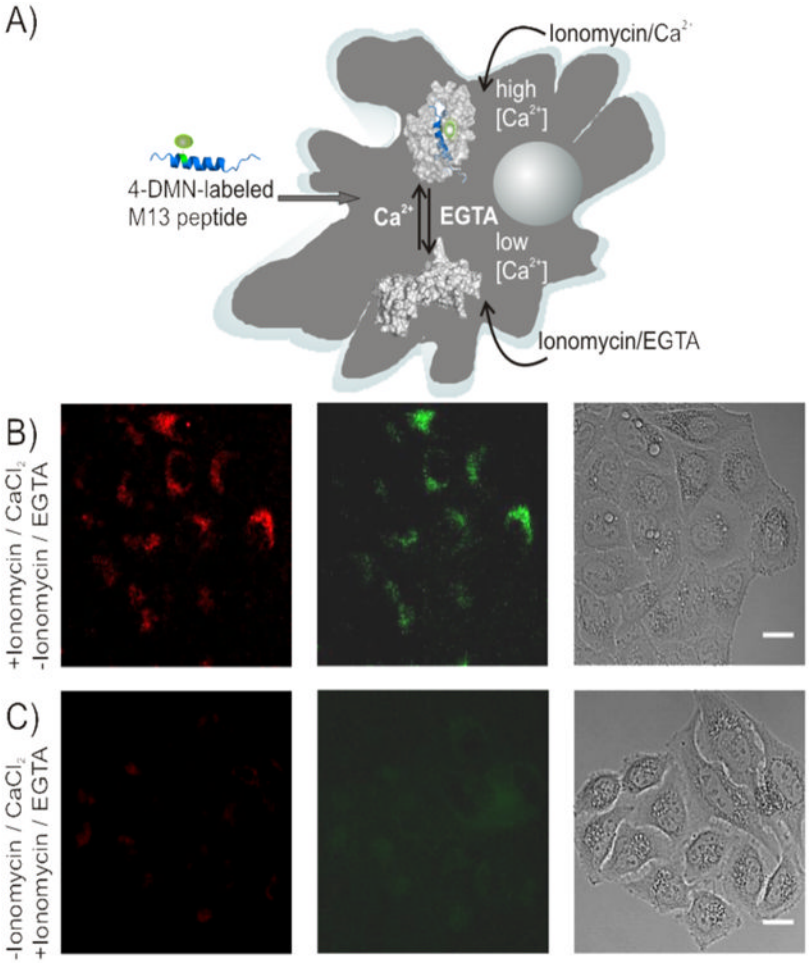

Figure 9.

Schematic of the system for image-based detection of endogenous CaM employing the 4-DMN-labeled M13 peptide. The M13 peptide sequence is predicted to penetrate through the plasma membrane as it has a high relative abundance of positively charged amino acids (7 out of 18). Due to the Ca^{2+} induced interaction of the 4-DMN-labeled M13 peptide and CaM the fluorescence increases. The fluorescence can be decreased by addition of EGTA which consequently reduces the concentration of Ca^{2+}. Two-photon excitation fluorescence (left), one-photon excitation fluorescence (center) and bright-field images (right) of living HeLa cells. The fluorescence images show the detection of endogenous CaM with 4-DMN-labeled M13 peptide incubated overnight, B) after addition of inomycin/Ca^{2+}, and C) after addition of ionomycin/EGTA. Scale bar, 20 μm.

Table 1

Two-photon cross-sections for 4-DMN-CaM systems at 800 nm excitation.

Sample	δ (GM)	Enhancement from DMF
4-DMN (DMF)	4.6	1.00
4DMN-M13 + EGTA	1.3	0.29
4DMN-M13 + Ca^{2+}	1.1	0.23
E11C + EGTA	5.1	1.10
E11C + Ca^{2+}	4.9	1.07
S38C + EGTA	40.5	8.80
S38C + Ca^{2+}	22.6	4.92

Table 2

Quantum yield of CaM-4-DMN derivatives under calcium-free and calcium-bound conditions (30% of given quantity). The ratio of respective quantum yields is also shown.

Quantum Yield (ϕ)	**M13**	**E11C**	**S38C**
CaM-4DMN + EGTA	0.003	0.007	0.002
CaM-4DMN + Ca^{2+}	0.193	0.059	0.26
ratio of quantum yields			
CaM-4DMN + EGTA/CaM-4DMN + Ca^{2+}	**64.20**	**8.58**	**130.00**

Table 3

Summary of time-correlated single photon counting decay lifetimes at 420 nm excitation and 500 nm detection. For double exponential decays relative component's amplitudes are shown in parenthesis.

Sample	Fluorescence Lifetime (ns)	Anisotropy Lifetime (ns)
4-DMN (DMF)	8.2	<1
4-DMN-S38C-CaM + EGTA	0.064(0.985), 2.31(0.015)	1.8 (0.83), 17.3 (0.16)
4-DMN-S38C-CaM + Ca2+	10.2	13.3